Prediction of the Nocturnal Surface Inversion Height[1]

TETSUJI YAMADA

Atmospheric Physics Section, Radiological and Environmental Research Division, Argonne National Laboratory, Argonne, IL 60439

(Manuscript received 25 May 1978, in final form 22 December 1978)

ABSTRACT

A simple prognostic equation for predicting the development of the nocturnal surface inversion height is constructed from the thermal energy equation. The purpose of the paper is to provide a simple method to estimate the nocturnal surface inversion heights to augment the prediction of the mixed-layer heights (Yamada and Berman, 1979) for regional-scale pollutant dispersion models. A significant improvement of the present model over previous simple models is the inclusion of atmospheric cooling due to longwave radiation. Another important difference, which considerably simplifies the present model, is the adoption of an empirical expression for the potential temperature profile. Predictions agree quite well with the data of the Wangara experiment.

1. Introduction

The planetary boundary layer (PBL) height, defined as the maximum vertical extent at which surface effects are still perceived, varies diurnally from less than 500 m during the night to over 1000 m during the day. Differences in boundary layers from day to night appear not only in height but also in dynamic structure. For example, vertical mixing due to turbulence within the nocturnal boundary layer is much less than that during daytime, due to the effects of negative buoyancy associated with the nighttime surface temperature inversion. It is particularly important for prediction of pollutant dispersion to know the characteristics of the PBL during both day and night. The purpose of the paper is to provide a simple method to estimate the nocturnal surface inversion heights to augment the prediction of the mixed-layer heights (Yamada and Berman, 1979) for regional-scale pollutant dispersion models.

Although a number of methods for predicting daytime mixing-layer height can be found (e.g., Ball, 1960; Lilly, 1968; Betts, 1973; Tennekes, 1973), there are relatively few relationships for predicting the nocturnal surface inversion height. This is mainly due to the fact that the dynamical description of the convective[2] PBL can be considerably simplified, since the vertical profiles for both wind and potential temperature become almost uniform due to strong turbulent mixing. No such simplification is justified for the nocturnal PBL.

A recent paper by Yu (1978) examined existing diagnostic (Clarke, 1970; Deardorff, 1972; Businger and Arya, 1974; Zilitinkevich and Monin, 1974) equations used for prediction of the nocturnal surface inversion height. Although his findings are not conclusive, the tested diagnostic equations obtained satisfactory results only when the atmospheric stability was either very weak or very strong. Furthermore, predictions by the prognostic equations, in general, were found to be much poorer than those using the diagnostic equations.

This paper first reviews the formation and development of both the convective and nocturnal PBL's, then proposes a simple method to predict the development of the nocturnal surface inversion height. Predictions are compared with observations from the Wangara experiment (Clarke *et al.*, 1971).

2. Formation and development of the PBL

The nocturnal surface inversion height h for the ideal horizontally homogeneous atmosphere may be defined as the lowest height where the temperature lapse rate changes to the dry adiabatic. However, for less ideal conditions h is determined as the height to which significant cooling had extended (Melgarejo and Deardorff, 1974). This is illustrated in Fig. 1a; a potential temperature profile in the PBL, almost uniform with height prior to sunset, indicates the formation of a surface inversion layer at a height $h_i(t_1)$, as the surface temperature decreases slightly to $T_s(t_1)$ due to longwave radiative cooling at the surface. As the surface temperature decreases further, the temperature in the layer above the surface decreases due to downward heat transfer by turbulence and cooling due to long-

[1] Work performed under the auspices of the U. S. Department of Energy.

[2] The word convective is used interchangeably with daytime in this study.

0021-8952/79/040526-06$05.50
© 1979 American Meteorological Society

Unauthenticated | Downloaded 07/28/21 05:46 PM UTC

wave radiation. Consequently, the surface inversion height increases to $h_i(t_2)$ and continues to grow until the surface temperature reaches a minimum value just before radiation sunrise (t_3). As the sun rises the surface temperature increases to $T_s(t_4)$ as shown in Fig. 1b, resulting in a convective mixing layer of height $h_c(t_4)$ capped by the nocturnal inversion. Penetration into the inversion is often observed. As the surface temperature continues to increase, so does the convective layer height $h_c(t_5)$ and the nocturnal inversion layer completely disappears by time t_6. Thereafter the mixing layer grows very rapidly (several hundred meters per hour) and reaches the upper inversion $h_c(t_7)$ in a short time as the surface temperature continues to increase. Once the convective layer reaches the upper inversion it grows much more slowly. After sunset the nocturnal surface inversion begins to re-form as discussed above. Fig. 2 depicts the evolution of both nocturnal and convective PBL heights determined from Figs. 1a and 1b. The present discussion, however, is limited to the development of the nocturnal surface inversion layer during the period extending from a few hours after sunset until sunrise.

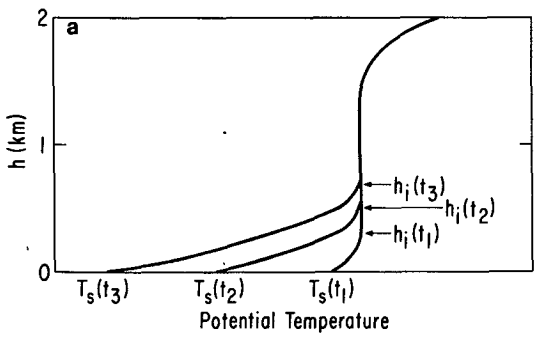

FIG. 1a. Typical development of the nocturnal surface inversion layer h_i.

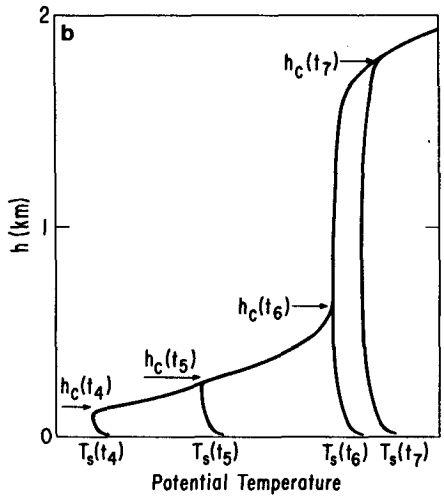

FIG. 1b. Typical growth of the convective mixing layer h_c.

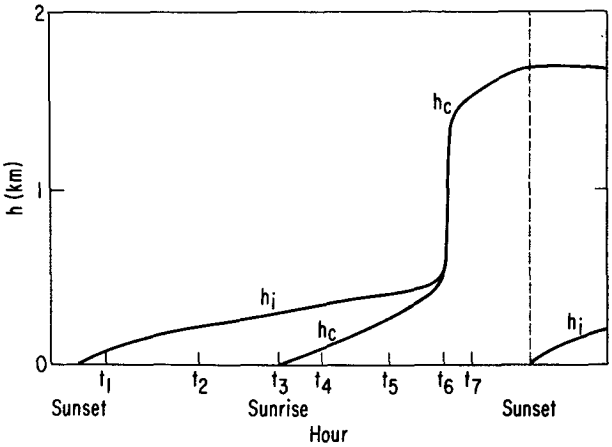

FIG. 2. Typical diurnal variations of the nocturnal surface inversion h_i and the convective mixing layers h_c constructed from Figs. 1a and 1b.

3. A predictive equation

The purpose of this study is to develop a simple method to predict the development of the nocturnal surface inversion height. It should be noted that the present method may be applied only where horizontal homogeneity is approximately satisfied. Thus, both vertical and horizontal transport terms are omitted in the model equation discussed below. For more general conditions appropriate numerical models (e.g., Yamada, 1978) may be used to predict the nocturnal (as well as convective) boundary layer height; however, a simple method for prediction of the PBL height is particularly valuable for simple operational air pollution prediction models.

A growth rate equation for the nocturnal surface inversion layer may be constructed from the thermal energy equation for flat terrain

$$\frac{\partial \Theta}{\partial t}=\frac{\partial}{\partial z}(-\overline{w\theta})+\left(\frac{\partial \Theta}{\partial t}\right)_r, \tag{1}$$

where t is time, z the vertical coordinate, Θ and θ the mean and fluctuation values of potential temperature, respectively, $-\overline{w\theta}$ the turbulent heat flux,[3] w the fluctuation of vertical motion, and $(\partial\Theta/\partial t)_r$ the rate of changes of the atmospheric temperature due to longwave radiation.

Integration of (1) from $z = 0$ to the top of the surface inversion height h yields

$$\int_0^h \frac{\partial \Theta}{\partial t}dz=(\overline{w\theta})_s-(\overline{w\theta})_h+\int_0^h \left(\frac{\partial \Theta}{\partial t}\right)_r dz, \tag{2}$$

[3] For simplicity $-\overline{w\theta}$ is referred to as the turbulent heat flux in this study although the correct heat flux should be $-\rho c_p \overline{w\theta}$ where ρ is the air density and c_p the specific heat of air at constant pressure.

Unauthenticated | Downloaded 07/28/21 05:46 PM UTC

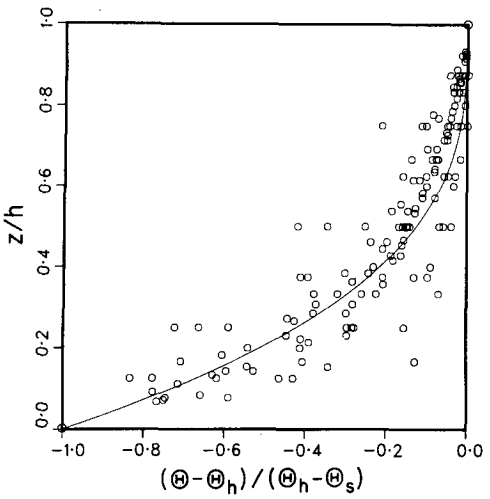

FIG. 3. Normalized potential temperature profiles for the nocturnal boundary layer data from Nights 11, 13, 30, 31 and 33 of the Wangara experiment. Subscripts h and s indicate the values at the surface inversion height and at the surface, respectively. Height is normalized by the surface inversion height h. A solid line represents $(\Theta-\Theta_h)/(\Theta_h-\Theta_s)=-(1-z/h)^3$.

where the subscripts s and h refer to the values at the surface[4] and at $z=h$, respectively. The left-hand side of Eq. (2) may be rewritten by using Leibniz's rule for interchanging the order of differentiation and integration. Thus,

$$\text{LHS}=\frac{\partial}{\partial t}\int_0^h \Theta dz-\Theta_h\frac{dh}{dt}. \tag{3}$$

A simple, empirical expression for the vertical profile of potential temperature is assumed, i.e.,

$$\frac{\Theta-\Theta_h}{\Theta_h-\Theta_s}=-\left(1-\frac{z}{h}\right)^3, \tag{4}$$

which enables us to perform the integration of Θ in (3). This relation is determined from Fig. 3, which shows normalized potential temperature profiles taken from the Wangara data. In general, the profile as given by (4) may also be a function of atmospheric stability, for example, h/L, where L is the Obukhov length. Thus, large variations depicted in Fig. 3 may be partially due to the fact that data under various stability conditions are included. However, classifications of the profiles by h/L was not possible since the data necessary to compute L were not listed[5] in the Wangara report. On the other hand, Clarke (1970) has found from analyses of the "pre" Wangara experiment that normalized potential temperature profiles are almost exactly proportional to $(zf/u_*)^{-1}$, when $zf/u_*\gtrsim 0.08$, where f is the Coriolis parameter and u_* the friction velocity.

[4] Surface refers to a screen height (~1.2 m).

[5] Mr. B. Hicks (personal communication) of Argonne National Laboratory is recomputing the surface heat flux and momentum flux for the Wangara experiment.

If a relation $z/h=\alpha(zf/u_*)$, where $0.1<\alpha<0.4$, is assumed, Clarkes relation should be valid for $z/h>0.4$ ($\alpha=0.2$ is used) in Fig. 3. However, the data shown in Fig. 3 do not justify expressions more complex than (4) because of the ambiguity in determining nocturnal surface inversion heights from the observed potential temperature profiles. The readers should be cautioned that the cubic temperature profile [Eq. (4)] appears to be supported by the Wangara data as shown in Fig. 3 but may not be applicable to the data obtained at different locations. A simple power profile for the potential temperature was chosen so that the integration

$$\int_0^h \Theta dz$$

can be performed easily. The cubic curve [Eq. (4)] does not match with the familiar log-linear profile in the surface layer and tends to deviate from the data in the region $z/h>0.5$ (Fig. 3). However, the area under the cubic curve agrees within 5% of error with the area integrated graphically. Now it is possible to perform the integration

$$\int_0^h \Theta dz$$

in (3) by using the assumed profile (4). The result is

$$\text{LHS}=\frac{\partial}{\partial t}\left[\tfrac{1}{4}(3\Theta_h+\Theta_s)h\right]-\Theta_h\frac{dh}{dt}$$

$$=\left[\tfrac{1}{4}(\Theta_s-\Theta_h)\right]\frac{dh}{dt}+\frac{h}{4}\left(3\frac{\partial\Theta_h}{\partial t}+\frac{\partial\Theta_s}{\partial t}\right). \tag{5}$$

Since turbulence in the nocturnal boundary layer decreases rapidly with height, Eq. (1) at $z=h$ becomes

$$\left(\frac{\partial\Theta}{\partial t}\right)_r=\frac{\partial\Theta_h}{\partial t}. \tag{6}$$

On the other hand, the air at the surface and very close to the surface is cooled, when turbulence is small, by longwave radiation during the night, and Eq. (1) in this layer becomes

$$\left(\frac{\partial\Theta}{\partial t}\right)_r=C\frac{\partial\Theta_s}{\partial t}, \tag{7}$$

where a constant C ($=1$) is introduced to conveniently identify the radiative cooling term in the later analyses. Eq. (7) may be supported by evaluating the order of magnitudes of the terms in Eq. (1). As a first approximation the turbulent heat flux is assumed to vary linearly with height and vanish at h. Thus, $-\partial(\overline{w\theta})/\partial z=(\overline{w\theta})_s/h=2\times10^{-5}$ s^{-1} °C where $(\overline{w\theta})_s=-0.008$°C m s^{-1} (as used in the later analyses) and $h=400$ m (see Fig. 4) are

Unauthenticated | Downloaded 07/28/21 05:46 PM UTC

substituted. On the other hand, $\partial\Theta_s/\partial t$ is typically $-10°C(10\text{ h})^{-1}$ [2.8×10^{-4} $s^{-1}°C$] which is one order of magnitude greater than $-\partial(\overline{w\theta})/\partial z$. The constant C could be less than unity to retain the effects of turbulence. However, the best results were obtained with $C=1$. The simplest expression to satisfy both (6) and (7) is a linear interpolation given by

$$\left(\frac{\partial\Theta}{\partial t}\right)_r = C\frac{\partial\Theta_s}{\partial t}\left(1-\frac{z}{h}\right)+\frac{\partial\Theta_h}{\partial t}\frac{z}{h}. \tag{8}$$

The radiative cooling rate is found to be maximum at approximately 5 cm above the surface (e.g., see Fleagle and Businger, 1974, p. 200; Kondo, 1971) and approaches a small value as height increases. On the other hand, radiative heating is found in a very thin layer (~3 cm) just above a wet surface. However, it is not necessary in this study to know an exact profile for the radiative cooling since, as seen in (2), only the result integrated vertically from the surface to the top of the surface inversion is required. Obviously, radiational heating confined in a thin layer of 3 cm responds very little to the integration over a 200 m layer. For this reason Eq. (8) appears to be an adequate approximation. Substituting (8) into (2), the right-hand side (RHS) of (2) becomes

$$\text{RHS}=(\overline{w\theta})_s-(\overline{w\theta})_h+\frac{Ch}{2}\frac{\partial\Theta_s}{\partial t}+\frac{h}{2}\frac{\partial\Theta_h}{\partial t}. \tag{9}$$

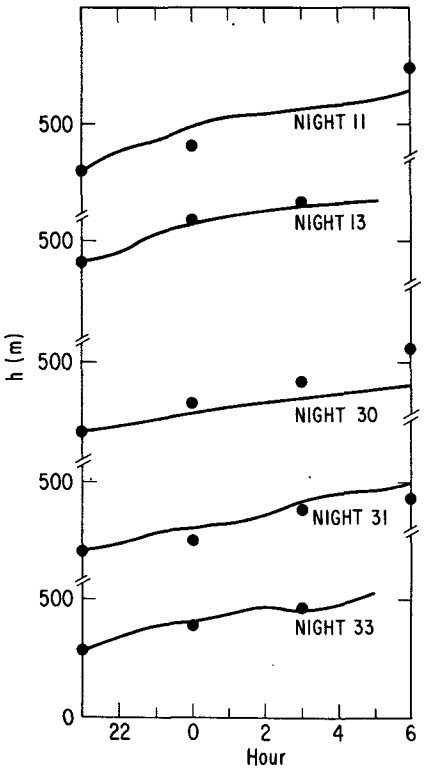

FIG. 4. Predicted and observed nocturnal surface inversion heights for Nights 11, 13, 30, 31 and 33.

Equating (5) and (9) we obtain a growth rate equation for h:

$$\frac{dh}{dt}=\frac{-1}{\Theta_h-\Theta_s}\left\{2Ch\frac{\partial\Theta_s}{\partial t}-h\left(\frac{\partial\Theta_s}{\partial t}+\frac{\partial\Theta_h}{\partial t}\right)+4[(\overline{w\theta})_s-(\overline{w\theta})_h]\right\}. \tag{10}$$

A typical value for $\partial\Theta_h/\partial t$ is of the order of 2°C day^{-1}. This is almost one order of magnitude smaller than $\partial\Theta_s/\partial t$, being typically 24°C day^{-1} (or a temperature decrease of the order of 10°C in 10 h between sunset and sunrise) obtained from the Wangara data. Turbulent heat flux in the nocturnal boundary layer decreases very rapidly with height and monotonically approaches zero. Therefore, a further simplification of (10) may be made by omitting $(\overline{w\theta})_h$ and $\partial\Theta_h/\partial t$ compared with $(\overline{w\theta})_s$ and $\partial\Theta_s/\partial t$, respectively. The final expression is

$$\frac{dh}{dt}=\frac{-1}{\Theta_h-\Theta_s}\left[2Ch\frac{\partial\Theta_s}{\partial t}-h\frac{\partial\Theta_s}{\partial t}+4(\overline{w\theta})_s\right], \tag{11}$$

where $C=1$.

4. Comparison with data

Surface inversion heights predicted by numerically integrating (11) have been compared with selected cases from the Wangara experiment. The Wangara data include temperature profiles, observed every 3 h with vertical resolution of 50 m for the first 1000 m above the surface, from which the heights of the surface inversion can be determined. The surface temperature in (11) is approximated by the screen-height temperature, which was measured hourly. For small h (say, $h\approx10$ m), Eq. (11) may be approximated by

$$dh/dt \approx 4ku_*/[\ln(h/z_0)-\psi], \tag{12}$$

where u_* is the friction velocity, k von Kármán's constant, z_0 the thermal roughness length and ψ the correction for the atmospheric stability (Panofsky, 1963). For deriving (12) the relationship

$$(\Theta_h-\Theta_s)/T_*=(1/k)[\ln(h/z_0)-\psi] \tag{13}$$

is used where T_* is the friction temperature. Therefore, Eq. (12) may be used for predicting the initial development of the nocturnal surface inversion layer, if measurements of the turbulent fluxes at the surface with sufficient time resolution are available. The Wangara report, however, did not list the surface turbulent fluxes during nighttime. Indirect estimates (Yamada and Mellor, 1975; Yamada 1976) indicate that the surface heat flux decreases rapidly after sunset but remains approximately constant (-0.008°C m s^{-1}) after 2100 Local Standard. Therefore, this study addresses the prediction of the surface inversion height only after 2100

Unauthenticated | Downloaded 07/28/21 05:46 PM UTC

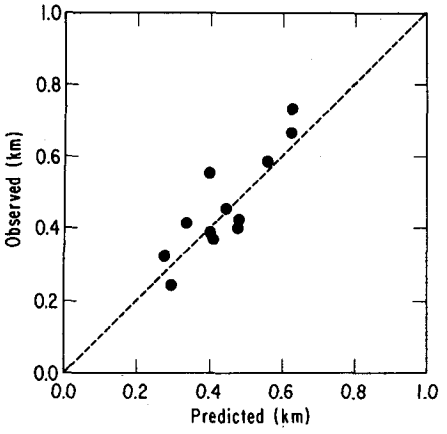

FIG. 5. Comparison of the observed and predicted nocturnal surface inversion heights.

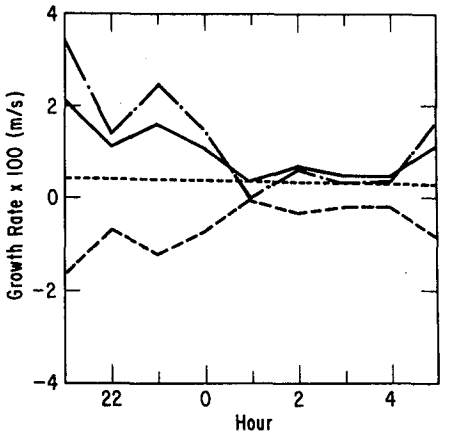

FIG. 6. Hourly variation of the terms in the growth-rate equation (11) for Night 11. The curves represent the terms related to the longwave radiation $[-2Ch(\partial\Theta_s/\partial t)/(\Theta_h-\Theta_s)]$ (— — —), the turbulent heat flux $[-4(\overline{w\theta})_s/(\Theta_h-\Theta_s)]$ (- - - - - -), the surface temperature variation $[h(\partial\Theta_s/\partial t)/(\Theta_h-\Theta_s)]$ (— — —) and the total growth-rate of the nocturnal surface inversion layer $[dh/dt]$ (———).

by using Eq. (11). It is assumed that the surface heat flux[6] (-0.008°C m s^{-1}) remain unchanged during Nights 11,[7] 13, 30, 31 and 33 for which observations and predictions are compared. The nocturnal surface inversion heights during these periods are relatively easily determined from the data. Development of the predicted and observed nocturnal inversion heights for each night are shown in Fig. 4 and summarized in Fig. 5. The boundary-layer heights initially grow relatively rapidly but the growth rates appear to decrease with time, typically reaching approximately 30 m h^{-1} by 0500 LST. In general, agreement between predictions and observations is good; differences are usually within 50 m.

Fig. 6 shows the hourly variations of each term in the growth-rate equation (11) for Night 11. As expected, the main positive contribution to the growth rate is the radiation term $-2Ch(\partial\Theta_s/\partial t)/(\Theta_h-\Theta_s)$, while the term due to the turbulent heat flux $-4(\overline{w\theta})_s/(\Theta_h-\Theta_s)$ makes a small contribution. Counter-contributions for the first few hours are mainly from the term related to the surface temperature variation $h(\partial\Theta_s/\partial t)/(\Theta_h-\Theta_s)$. It is also evident that the growth rate correlates very well with the term involving the surface temperature variations, which is not surprising since the parameterization of radiative cooling include the surface temperature variations [see Eq. (8)].

5. Summary and remarks

A simple prognostic equation is proposed to provide the nocturnal surface inversion heights for regional-scale pollutant transport models. A significant improvement of the present model over previous simple models for the prediction of nocturnal surface inversion heights is the inclusion of atmospheric cooling due to longwave radiation. A simple parameterization of the radiational effect and a simple cubic polynomial profile for the potential temperature, necessary to maintain model simplicity, appear to be sufficient for the present purpose. The latter assumption, however, may not be applicable to the data obtained at different locations. The agreement between the predictions and observations for five selected nights from the Wangara data is good; differences mostly are within 50 m. The derivation of the model assumes a horizontally homogeneous flow (no horizontal and vertical advections), and no entrainment at the top of the surface inversion. It is also assumed that the local change of the potential temperature at the top of the surface inversion is small compared to that in the surface layer and can be neglected.

Acknowledgments. The author is grateful to Drs. R. Coulter, J. Shannon and J. Sheih who carefully read the manuscript and made useful suggestions. The author is also indebted to Mrs. R. Spencer for her excellent typing of the manuscript.

[6] According to Mr. B. Hicks (personal communication) analyses of the Wangara surface data yield an averaged surface heat flux during the period between 2100 and 0600 for the five nights tested (Fig. 5) of -0.008°C m s^{-1}.

[7] Night 11 refers to the night between Days 11 and 12, etc.

REFERENCES

Ball, F. K., 1960: Control of inversion height by surface heating. *Quart. J. Roy. Meteor. Soc.*, **86**, 483–494.

Betts, A. K., 1973: Non-precipitating cumulus convection and its parameterization. *Quart. J. Roy. Meteor. Soc.*, **99**, 178–196.

Businger, J. A., and S. P. S. Arya, 1974: Heights of the mixed layer in the stably stratified planetary boundary layer. *Advances in Geophysics*, Vol. 18A, Academic Press, 73–92.

Clarke, R. H., 1970: Observational studies in the atmospheric boundary layer. *Quart. J. Roy. Meteor. Soc.*, **96**, 91–114.

——, A. J. Dyer, R. R. Brook, D. G. Reid and A. J. Troup, 1971: The Wangara experiment: Boundary layer data. CSIRO Div. Meteor. Physics, Tech. Pap. No. 19, 336 pp.

Deardorff, J. W., 1972: Rate of growth of the nocturnal boundary

Unauthenticated | Downloaded 07/28/21 05:46 PM UTC

layer. *Preprints Symp. Air Pollution, Turbulence and Diffusion*, Las Cruces, Amer. Meteor. Soc., 183–190.

——, 1972: Parameterization of the planetary boundary layer for use in general circulation models. *Mon. Wea. Rev.*, **100**, 93–106.

Fleagle, R. G. and J. A. Businger, 1974: *An Introduction to Atmospheric Physics*. Academic Press, 346 pp.

Kondo, J., 1971: Effect of radiative heat transfer on profiles of wind, temperature and water vapor in the atmospheric boundary layer. *J. Meteor. Soc. Japan*, **49**, 75–94.

Lilly, D. K., 1968: Models of cloud-topped mixed layers under a strong inversion. *Bull. Amer. Meteor. Soc.*, **53**, 17–23.

Melgarejo, J. W., and J. W. Deardorff, 1974: Stability functions for the boundary-layer resistance laws based upon observed boundary layer height. *J. Atmos. Sci.*, **31**, 1324–1333.

Panofsky, H. A., 1963: Determination of stress from wind and temperature measurements. *Quart. J. Roy. Meteor. Soc.*, **23**, 495–502.

Tennekes, H., 1973: A model for the dynamics of the inversion above a convective boundary layer. *J. Atmos. Sci.*, **30**, 558–567.

Yamada, T., 1976: On the similarity functions A, B and C of the planetary boundary layer. *J. Atmos. Sci.*, **33**, 781–793.

——, 1978: A three-dimensional, second-order closure numerical model of mesoscale circulations in the lower atmosphere. Topical Rep. ANL/RER-78-1, Argonne National Laboratory, 67 pp.

——, and G. L. Mellor, 1975: A simulation of the Wangara atmospheric boundary layer data. *J. Atmos. Sci.*, **32**, 2309–2329.

——, and S. Berman, 1979: A critical evaluation of a simple mixed layer model with convective penetration (in press). *J. Appl. Meteor.*

Yu, T., 1978: Determining height of the nocturnal boundary layer. *J. Appl. Meteor.*, **17**, 28–33.

Zilitinkevich, S. S., and A. S. Monin, 1974: Similarity theory for the atmospheric boundary layer. *Izv. Akad. Nauk SSSR, Fiz. Atmos. Okeana.*, **10**, 587–599.

Unauthenticated | Downloaded 07/28/21 05:46 PM UTC